Competing magnetic phases in $La_{0.7}Sr_{0.3}MnO_3$ as deduced from Mn site hyperfine parameters

2006 J. Phys.: Condens. Matter 18 7651

(http://iopscience.iop.org/0953-8984/18/32/013)

INSTITUTE OF PHYSICS PUBLISHING JOURNAL OF PHYSICS: CONDENSED MATTER

J. Phys.: Condens. Matter **18** (2006) 7651–7658 doi:10.1088/0953-8984/18/32/013

Competing magnetic phases in $La_{0.7}Sr_{0.3}MnO_3$ as deduced from Mn site hyperfine parameters

R Govindaraj[1] **and C S Sundar**[1,2]

[1] Materials Science Division, Indira Gandhi Centre for Atomic Research, Kalpakkam-603 102, India
[2] Jawaharlal Nehru Center for Advanced Scientific Research, Bangalore-560 064, India

Received 5 June 2006
Published 31 July 2006
Online at stacks.iop.org/JPhysCM/18/7651

Abstract

Time differential perturbed angular correlation measurements using the ^{181}Ta probe in $La_{0.7}Sr_{0.3}Mn_{0.995}Hf_{0.005}O_3$ reveal the presence of two distinct hyperfine components, identified with probe atoms occupying Mn sites which are rich and deficient in hole concentration. The Mn^{4+} rich zones exhibit ferromagnetic ordering at all temperatures below 360 K, the bulk Curie temperature. In the case of Mn^{4+} deficient zones, the paramagnetic order is seen to evolve into a canted antiferromagnetic ordering below 360 K, that becomes ferromagnetic below 250 K. Concomitantly, there is a change in the fractions below 250 K. The implications of these results are discussed in terms of electronic phase separation.

Besides taking into account double exchange (DE) interaction and Jahn–Teller distortion, the phenomenon of colossal magneto-resistance (CMR) could be quantitatively explained only in terms of occurrence of multiple phases differing in hole concentration and with competing magnetic interactions [1–9]. The phase diagrams of these oxides, mostly deduced based on bulk magnetization, x-ray diffraction and transport properties, are rich and complicated due to a strong coupling between spin, charge, orbital and lattice degrees of freedom [1, 2, 4]. Even at a specific composition x in $La_{1-x}Sr_xMnO_3$, occurrence of nanoscopic inhomogeneous phases differing in local electrical, magnetic and structural properties have been reported [6, 7, 10, 11], which play a crucial role for understanding the CMR properties. These points emphasize the importance of understanding both the local electronic and magnetic properties of the competing phases existing in the system. This is possible by deducing hyperfine parameters such as magnetic hyperfine field (MHF) and electric field gradient (EFG) *at* Mn *sites*, as MnO_6 octahedra play a crucial role in magnetic and electronic properties of the corresponding phases present in the system. MHF is dependent upon the Mn spin ordering and EFG yields information about the local structural and electronic properties.

Hyperfine studies such as ^{55}Mn NMR [12] and ^{57}Fe Mossbauer [13] spectroscopy have been carried out in $La_{1-x}A_xMnO_3$ (A = Ca, Sr), bringing out the coexisting phases of varying

hole concentration exhibiting different magnetic ordering and signature of phase separations in these systems. However, a detailed picture involving the changes in both the MHF and EFG of the coexisting phases and hence the complete atomic scale understanding of these phases is yet to emerge. Using time differential perturbed angular correlation (TDPAC), a hyperfine interaction technique with ^{181}Hf/Ta probe, it has been shown that Hf substitutes Mn sites in undoped [14, 15] and Ca/Sr doped $LaMnO_3$ [16, 17]. The MHF as perceived by the probe nucleus (Ta) occupying Mn sites is due to the transfer of spin density from magnetically ordered Mn d orbitals through O p orbitals on to primarily the 4s and 5s orbitals of the probe ion, namely the super transferred hyperfine field (STHF). The EFG at the site of the probe nuclei depends upon the charge distribution of nearby oxygen ions, and hence is dictated by electronic and structural properties such as orientation of orbitals and distortions of nearby MnO_6 octahedra. It has been shown that Hf substitutes two distinct Mn sites, namely rich in Mn^{4+} and deficient in Mn^{4+}, in $La_{0.7}A_{0.3}MnO_3$ (A = Ca, Sr). In $La_{0.7}Sr_{0.3}MnO_3$, Mn^{4+} rich zones were observed to exhibit ferromagnetic while Mn^{3+} rich zones canted weak antiferromagnetic ordering in the temperature interval between 300 and 360 K [17]. Present measurements extended down to 10 K bring out interesting results of phase separation of CAFM to FM zones. This work also illustrates a linear correlation between EFG and MHF as experienced by probe atoms occupying Mn^{3+} and Mn^{4+} rich sites with the slope being dictated by the nature of local magnetic ordering.

$La_{0.7}Sr_{0.3}Mn_{0.995}Hf_{0.005}O_3$ (LSMO) samples were prepared by the standard solid state reaction method described elsewhere [16] and characterized by x-ray diffraction to be of single phase with rhombohedral structure having lattice parameters $a = 5.5032$ Å and $c = 13.375$ Å. These samples were neutron irradiated at the DHRUVA reactor, BARC, Mumbai, to produce the probe nuclei by the reaction $^{180}\mathrm{Hf}(n,\gamma)^{181}\mathrm{Hf}(\beta^-)^{181}\mathrm{Ta}$. These thermal neutron irradiated samples were annealed in air at 870 K for 30 min. The 133–482 keV γ–γ coincidences of the cascade in ^{181}Ta (separated by the isomeric state of $I = 5/2$ with nuclear moments, namely $\mu = 3.245\ \mu_N$ and $Q = 2.51$b) were measured using a three detector, twin fast–slow coincidence set-up, using BaF_2 detectors with a time resolution of 660 ps (FWHM). From the measured coincidence spectra obtained with detectors set for 482 keV γ rays at 90° and 180° with respect to the one set for 133 keV γ rays, namely $W(90°, t)$ and $W(180°, t)$, the anisotropy function $R(t) = 2[W(180°, t) - W(90°, t)]/[W(180°, t) + 2W(90°, t)]$ is evaluated [16], and this contains information on the hyperfine interaction parameters. This anisotropy function $R(t)$ is analysed to extract the quadrupole and magnetic hyperfine parameters: the Larmor frequency is given as $\omega_L = g\mu_N B_{hf}/\hbar$ where g is the nuclear gyromagnetic factor and B_{hf} is the MHF. The deduced quadrupole parameters are quadrupole frequency $\nu_Q = eQV_{zz}/h$ and asymmetry parameter $\eta = (V_{xx} - V_{yy})/V_{zz}$, where V_{xx}, V_{yy} and V_{zz} are the elements of the EFG tensor in its principal axis system. This analysis [18] also provides information on the fractions, f_i, of probe nuclei experiencing hyperfine frequencies, the angle β between B_{hf} and V_{zz}, and the width of the Lorentzian distribution of quadrupole frequencies, δ. Figure 1 shows a few representative anisotropy spectra and their Fourier transform for measurements carried out at different temperatures in LSMO. The spectra can be best fitted with only two fractions, both of them experiencing combined magnetic and quadrupole interactions below the bulk Curie temperature. This implies the presence of two distinct Mn sites in the matrix. Based on detailed PAC measurements on the aspects of ferromagnetic to paramagnetic phase transition, the effect of external magnetic field and oxygen stoichiometry effects, these sites are identified to be rich and deficient in Mn^{4+} [17]. The occurrence of such Mn^{3+} rich and Mn^{4+} rich zones have been identified in LCMO based on PAC studies related to oxygen stoichiometric effects. The existence of the two components in LSMO/LCMO has earlier been attributed to the intrinsic chemical inhomogeneity [16, 17, 19]

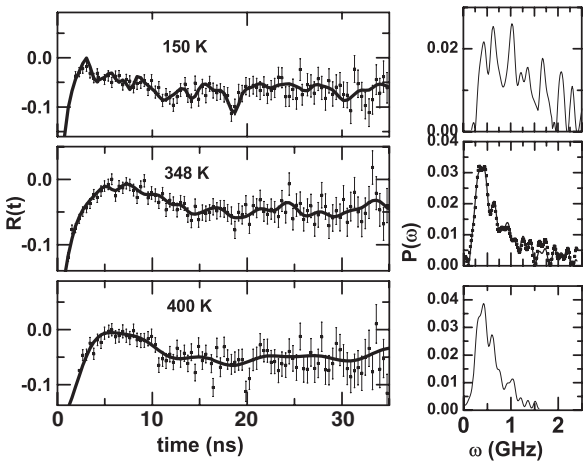

Figure 1. Representative TDPAC spectra in LSMO at different temperatures mentioned, across the ferromagnetic to paramagnetic phase transition. The continuous curve in each case represents the fit based on a two component model (see text). $P(\omega)$ corresponds to the Fourier transformed spectrum of each $R(t)$.

at the nanoscale arising due to Sr/Ca doping and the concomitant distribution of Mn^{4+} ions. Appreciable dampening of the spectra is mainly understood to be due to electronic inhomogeneity caused by the doping of Sr or Ca in these systems as discussed earlier [16]. The dampening parameter is significantly dependent upon cationic (La, Sr) and anionic (oxygen) concentration and distribution. In our earlier measurements we have illustrated an appreciable dependence of dampening on oxygen concentration [16, 17]. In addition, a small contribution to the dampening of the spectra by recoil induced defects of the constituent atoms (occupying next to next nearest neighbour surroundings of probe atoms) surviving the annealing treatment at 870 K could not be completely ruled out.

The results corresponding to FM–PM phase transition, in terms of the variation of hyperfine parameters corresponding to probe atoms associated with Mn^{3+} rich and Mn^{4+} rich zones, are shown in figures 2 and 3 respectively. It is seen from figure 2 that just below the bulk Curie temperature the value of ω_{L1} is close to 275 MHz. In the temperature interval between 360 and 300 K, ω_{L1} reaches a maximum value of about 300 MHz, which is much smaller than that of ω_{L2} just above the bulk T_c of the sample. The variation of ω_{L1} is sluggish in the temperature interval, implying that the Mn spins in the Mn^{3+} rich zones are canted anti-ferromagnetically ordered [20]. This is consistent with the result that for $x \approx 0.1$ the magnetic ordering associated with $La_{1-x}Sr_xMnO_3$ is canted antiferromagnetic [24]. The top panel of figure 2 plotted between $\log(\omega_{L1})$ and $(1 - T/T_c)$ shows that there exist two slopes. A change in the slope or equivalently a discontinuity is seen around 250 K in the variation of ω_{L1}. In the temperature range between 250 and 10 K, it can be seen that the change in the Larmor precession frequency ω_{L1} is appreciably higher. It is understood that the spins of Mn in the Mn^{3+} rich zones become ferromagnetic from canted antiferromagnetic. This is in agreement with the reported results [24] that the ground state for $x \approx 0.1$ corresponds to the ferromagnetic insulating phase and the excited phase in which the ordering of Mn spins becomes canted antiferromagnetic. Concomitantly there is an appreciable variation of ν_{Q1} in the temperature interval 250–10 K. The angle between the principal component of the EFG and the direction of the magnetic field remains constant around 55° as seen in the figure.

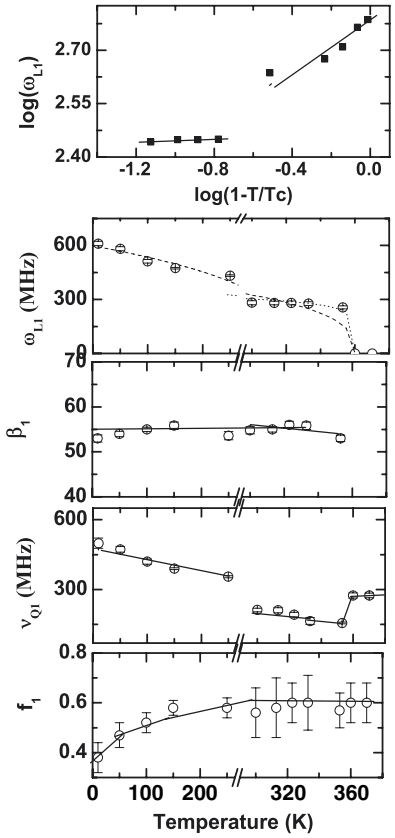

Figure 2. Variation of hyperfine parameters corresponding to probe atoms associated with Mn^{3+} rich zones across the ferromagnetic to paramagnetic transition in $La_{0.7}Sr_{0.3}Mn_{0.995}Hf_{0.005}O_3$.

The value of ω_{L2} lies between 500 MHz just below T_c and reaches as high as a value of 1700 MHz around 10 K. The top panel in figure 3 shows the variation of $\log(\omega_{L2})$ with $\log(1 - T/T_c)$. We have shown that the Mn^{4+} rich zones are ferromagnetic based on the PAC measurements carried out under the application of external magnetic field, vacuum quenching and oxygen annealing measurements [17]. This shows that the spins of Mn in Mn^{4+} rich regions remain ferromagnetic throughout the paramagnetic to ferromagnetic transition. A significant increase in ν_{Q2} has been observed concomitant to the variation of ω_{L2} below T_c. β_2 significantly increases from 60° just below T_c and saturates at a value of 80° below 250 K. f_1 and f_2 remain constant from 400 to 250 K, and below 250 K there is an increase in f_2 at the cost of f_1. This implies that the electronic phase separation effects are operative below 250 K.

Important and striking results of the present measurements are the following. (a) Variation of quadrupole frequency (ν_Q) similar to that of Larmor frequency (ω_L) corresponding to probe atoms occupying Mn sites that are Mn^{3+} rich and Mn^{4+} rich. (b) Observation of the change in magnetic ordering from canted weak AFM to ferromagnet associated with hole deficient regions below 250 K, as shown by a change of slope in $\log(\omega_{L1})$ versus $\log(1 - T/T_c)$ plot (cf figure 2). (c) This change in the magnetic ordering is observed to result in an increase in STHF (i.e ω_{L1}) and also in the value of EFG (i.e ν_{Q1}), thus resulting in a change of slope $(\Delta\nu_{Q1}/\Delta\omega_{L1})$ below 250 K. (d) There is no change in the magnitudes of the fractions around

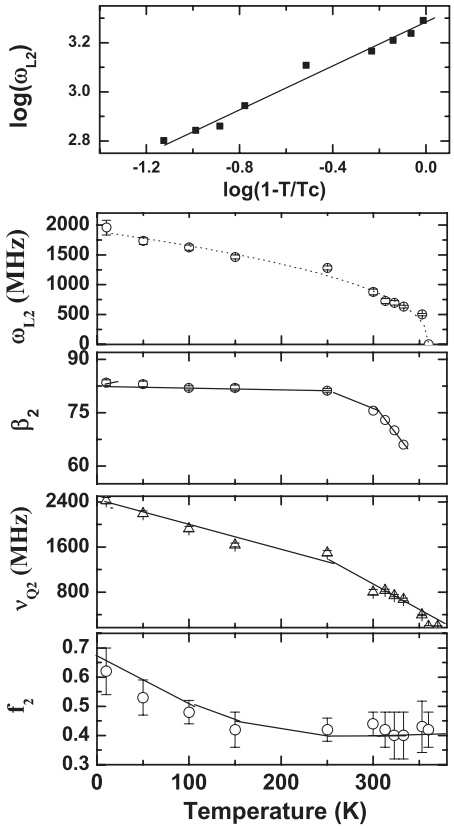

Figure 3. Variation of hyperfine parameters corresponding to probe atoms associated with Mn^{4+} rich zones across the ferromagnetic to paramagnetic transition in $La_{0.7}Sr_{0.3}Mn_{0.995}Hf_{0.005}O_3$.

the bulk ferromagnetic Curie temperature. But there is an increase of f_2 at the cost of f_1 below 250 K. (e) Above 360 K, there is a significant increase in ν_{Q1} while ν_{Q2} decreases steadily, similar to the variation in ω_{L2}. Detailed discussions of these observations are as follows.

The cause for a significant increase of ν_{Q2} below T_c (cf figure 3) has been discussed in our earlier work [17]. As EFG is proportional to $\langle q \rangle / r^3$, where $\langle q \rangle$ is the effective charge and r is the bond length, the observed increase could not be explained by taking into account magnetostriction effects [21] alone but only by invoking the changes in the charge distribution itself. Variation of quadrupole frequency versus Larmor precession frequency corresponding to Mn^{4+} rich and deficient zones in LSMO are shown in figure 4. The value of $\Delta\nu_{Q2}/\Delta\omega_{L2}$ is $\approx$1.5, while $\Delta\nu_{Q1}/\Delta\omega_{L1}$ takes a value of 0.42 in the range 300–350 K and a value of 1.5 below 250 K. ω_{L1} increases sharply below 250 K (cf figure 2), which is understood to be due to the canted weak antiferromagnetic to ferromagnetic transition. On comparison of the values of the slope $\Delta\nu_Q/\Delta\omega_L$ corresponding to different zones, it could be observed that the value of the slope is mainly dependent upon the nature of magnetic ordering. Ferromagnetic zones are seen to exhibit a high value of $\Delta\nu_Q/\Delta\omega_L$ around 1.5, while the value at canted AFM zones remains as low as 0.42. FM zones show orbital disordering with equal populations of $d_{x^2-y^2}$ and $d_{3z^2-r^2}$ orbitals while CAFM zones have the higher population of $d_{x^2-y^2}$ than $d_{3z^2-r^2}$ as discussed earlier [22]. A sharp change of ω_{L1} below 250 K is accompanied by a significant change in the slope $\Delta\nu_{Q1}/\Delta\omega_{L1}$, which is understood to be caused by the change in

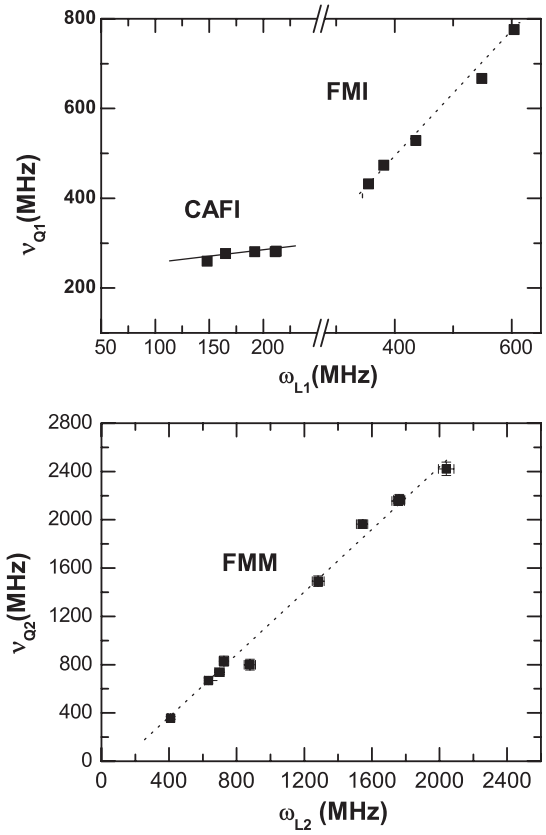

Figure 4. Linear correlation between the Larmor frequencies ω_{L1} and ω_{L2} with respective quadrupolar frequencies ν_{Q1} and ν_{Q2} in LSMO.

magnetic ordering. Since there is a concomitant change in the values of fractions below 250 K, it is interpreted that the above change in magnetic ordering could be caused by the electronic phase separation. An increase in the mobile hole concentration with lowering temperature is expected based on the double exchange mechanism of the manganites. Thus electronic phase separation in addition to temperature effects is expected to result in an increase in the mobile hole concentration in the Mn^{3+} rich zones. This leads to an increase in the orbital disordering causing a change from canted weak antiferromagnetic to ferromagnetic ordering. It has been predicted theoretically by de Gennes [23] that an increasing concentration of mobile holes would drive the system from canted antiferromagnetic structure to a metallic and ferromagnetic ground state. Our results that the ordering of Mn spins at hole deficient zones change from canted weak antiferromagnetic to ferromagnetic below 250 K are quite consistent with the bulk phase diagram obtained for $La_{1-x}Sr_xMnO_3$ with $x \approx 0.1$. It is shown that for $x \approx 0.08$, the system remains CI, which becomes ferromagnetic and insulating with the doping of holes [24–27]. Similar to the phase diagram, increase in the mobile hole concentration leads to doping of holes in the Mn^{3+} zones, resulting in the disordering of the orbitals. This in turn results in the ferromagnetic ordering of Mn spins. This effect is similar to that seen in the bulk $R_{1-x}A_xMnO_3$ with increasing x [24].

The present results, namely the change of magnetic ordering from CAFM to FM and the value of $\Delta\nu_Q/\Delta\omega_L$ being around 1.5, strongly suggest that in the zones scanned by f_1 DE interaction becomes more predominant than the superexchange interactions below 250 K. Based on these results we predict that the orbitals corresponding to Mn^{3+} rich zones below 250 K should be almost the same as that of Mn^{4+} zones with disordered configurations, with of course a smaller hole concentration than that corresponding to f_2. Linear correlation between MHF and EFG has been observed in systems such as $GdAl_2$ [28]. In the present study, the importance of orbital ordering, non-spherical charge distribution and spin–orbital coupling has been emphasized for the understanding of the strong correlation between EFG and MHF observed in the hole rich zones of LSMO [17, 29]. In the case of LCMO it is seen that the values of $(\Delta\nu_Q/\Delta\omega_L)$ remain as 0.12 and 1.5 respectively for hole deficient and hole rich zones respectively [29]. This is consistent with our results implying that the value of the slope is mainly dictated by the degree of spin ordering. Since CAFM is due to a competition between ferro- and antiferromagnetic ordering the value corresponding to this zone lies around 0.42.

It can be seen from figures 2 and 3, that the value of ν_{Q1} increases sharply and ν_{Q2} remains constant at a value of 150 MHz while the sample transits to paramagnetic state. At the paramagnetic state there is a significant static Jahn–Teller distortion associated with Mn^{3+} rich sites. A sharp increase in ν_{Q1} beyond T_c is essentially attributed to structural and electronic effects associated with Jahn–Teller distortion at Mn^{3+} rich sites. In the PM state the value of f_1:f_2 is in the ratio of $\approx$0.6:0.4 in Sr doped sample. It was earlier reported that the ratio is similar in the case of the Ca doped sample [16]. This implies that the occurrence of hole rich and hole deficient zones is mainly due to cationic inhomogeneity. These act as nucleating centres for the growth of hole rich and hole deficient zones in the sample due to electronic phase separation. The CAFM observed here is due to a strong competition between orbital ordering inducing AFM and orbital disordering and double exchange (DE) favouring ferromagnetic ordering.

Summarizing, the hole rich and hole deficient zones as observed above the Curie temperature are mainly understood to be due to cationic inhomogeneity at the nanoscale. Further, this experiment shows that in LSMO the phase separation effects are absent near the ferromagnetic to paramagnetic Curie temperature. But it is seen that the electronic phase separation effects occur as indicated by an increase in f_2 at the cost of f_1 below 250 K. Mn^{4+} rich regions remain ferromagnetically ordered below 360 K. Mn^{4+} deficient zones exhibit canted weak antiferromagnetic ordering below 360 K, which becomes ferromagnetic below 250 K. This change in the magnetic ordering in hole deficient zones could be due to electronic phase separation effects. This letter also brings out a very important linear correlation between EFG and MHF present universally in doped manganites with the values of slope determined predominantly by the nature of spin ordering and hence the spin–orbital interaction that exists in hole rich, deficient zones in the samples. Further, a significant increase in the quadrupole frequency associated with Mn^{4+} deficient zones above T_c is understood to be due to electronic and structural effects associated with Jahn–Teller distortion.

References

[1] Ramirez A P 1997 *J. Phys.: Condens. Matter* **9** 8171
[2] Salamon M B and Jaime M 2001 *Rev. Mod. Phys.* **73** 583
[3] Goodenough J B 1955 *Phys. Rev.* **100** 564
[4] Tokura Y and Nagosa N 2000 *Science* **288** 462
[5] Dagotto E, Hotta T and Moreo A 2001 *Phys. Rep.* **344** 1
[6] Dagotto E 2005 *New J. Phys.* **7** 67
[7] Ueharra M *et al* 1999 *Nature* **399** 560

[8] De Teresa J *et al* 1997 *Nature* **386** 256
[9] Milward G C, Calderon M J and Littlewood P B 2005 *Nature* **433** 607
[10] Radelli P G *et al* 2001 *Phys. Rev.* B **63** 172419
[11] Argyriu D N *et al* 2002 *Phys. Rev. Lett.* **89** 036401
[12] Savosta M M and Novak P 2001 *Phys. Rev. Lett.* **87** 137204
[13] Chechersky V *et al* 2000 *Phys. Rev.* B **62** 5316
[14] Catchen G L, Evenson W E and Alfred D 1996 *Phys. Rev.* B **54** R3679
[15] Rasera R L and Catchen G L 1998 *Phys. Rev.* B **58** 3218
[16] Govindaraj R *et al* 2004 *Chem. Phys.* **302** 185
[17] Govindaraj R and Sundar C S 2004 *Phys. Rev.* B **70** 220405
[18] Lindgren B 1996 *Hyperfine Interact.* C **1** 613
[19] Shibata T *et al* 2002 *Phys. Rev. Lett.* **88** 207205
Burgy J *et al* 2001 *Phys. Rev. Lett.* **87** 277202
[20] Zheludev A *et al* 1998 *Phys. Rev.* B **57** 2968
[21] Huang Q, Santoro A, Lynn J W, Erwin R W, Borchers J A, Peng J L, Ghosh K and Greene R L 1998 *Phys. Rev.* B **58** 2684
[22] Fang Z, Soloveyev I V and Terakura K 2000 *Phys. Rev. Lett.* **84** 3169
[23] de Gennes P G 1960 *Phys. Rev.* **118** 141
[24] Paraskevopoulos M, Mayer F, Hamburger J and Loidl A 2000 *J. Phys.: Condens. Matter* **12** 3993
[25] Zhou J S *et al* 1997 *Phys. Rev. Lett.* **79** 3234
[26] Urushibara A *et al* 1995 *Phys. Rev.* B **51** 14103
[27] Liu G L, Zhou J S and Goodenough J B 2004 *Phys. Rev.* B **70** 224421
[28] Degani J and Kapkan N 1973 *Phys. Rev.* B **7** 2132
Also see Bauer M *et al* 1993 *Phys. Rev.* B **48** 1014
[29] Govindaraj R and Sundar C S 2004 *Solid State Phys.* **49** 37